

Original Article

# Use of Plastic Gears for Power Transmission in Low-Torque Robotics: Wear and Fatigue Analysis

Erick Samillan<sup>1</sup>, Yonix Vilca<sup>1</sup>, Jorge Apaza<sup>1</sup>, Gonzalo Pereyra<sup>1</sup>, Christofer Diaz<sup>1\*</sup>

<sup>1</sup>Universidad Nacional de San Agustín de Arequipa, Arequipa, Peru.

\*Corresponding Author : [cdiazar@unsa.edu.pe](mailto:cdiazar@unsa.edu.pe)

Received: 14 February 2026

Revised: 22 March 2026

Accepted: 24 April 2026

Published: 29 May 2026

**Abstract** - This work presents a theoretical methodology, in the form of a simulation, for evaluating a pair of plastic pinion-wheel gears intended for power transmission in low-torque robotics applications. The geometry of the gear pair is parameterized in CAD, and a polymeric or engineering material with traceable properties is selected, along with a FEM model that includes tooth-to-tooth contact. The wear of the gear is estimated from the contact variables using an Archard-type law, accompanied by a parametric analysis for tribological uncertainties. Flexural fatigue at the tooth root is studied using the Stress-Life (S-N) approach, which provides indicators of gear life.

**Keywords** - Plastic gears, Low-torque robotics, Finite element analysis, Bending fatigue.

## 1. Introduction

Lightweight robotics encompasses platforms (e.g., cobots, humanoids, and mobile robots) in which mobility, agility, and safety during interaction with the environment, and in many cases with humans, are prioritized; consequently, the design aims to reduce mass and inertia without sacrificing joint functionality [1]. The use of transmission gears is very common in many industries because it allows an increase in the available output torque due to their compact and controllable design. Regarding plastic gears, they are typically utilized for 'low torque' applications; in previous research, the operating point is 10-15 N·m, reaching a maximum limit of roughly 50 N·m. [2].

Polymer gears generally do not fail from static stress alone. Instead, their breakdown is caused by a combination of mechanical loads, friction, and rising temperatures. This interaction ultimately leads to fatigue and tooth fracture [3, 4]. The polymer gear depends on several properties like temperature, load duration, and humidity; consequently, this significantly affects its useful Life. Recent research shows that temperature and the counterface material affect the durability of the gear. In addition, some authors propose in-situ measurement in plastic gears under spectrum loads; in other words, variable torque is measured while the temperature is constantly registered. These studies indicate that, in comparison with real-world scenarios, measurements obtained under constant loads are less accurate. Furthermore, other wear studies demonstrate that for plastic gears manufactured via FDM/FFF, surface topography and the manufacturing process have a significant relation to damage

progression. In short, the manufacturing method has a major impact on the gear's friction behavior.

About software simulation, numerical analysis, and the tribology research view tooth interaction as an essential aspect, because it allows the calculation of local pressures, slip motion, and heat production, with gears as an important factor in evaluating the accumulated Damage associated with bending fatigue [3, 4]. Using contact analysis methods, we can observe in a better way the errors and how load distribution in helical and noncircular gears, allowing a better understanding of how load concentration mechanisms [7, 8]. Fatigue models reveal how finite element models, with experimental verification, allow more effective detection of the main damage mode in gear systems under specific working conditions [4]. In addition, it is relevant to know that gear defects depend on geometric parameters and angular parameters to detect faults in early stages [9], and for this reason, understanding contact and damage processes from the initial design phase is fundamental. Material selection is a decisive factor for reliability and service life. Materials such as PA66 GF30, a polyamide reinforced with 30% glass fiber, are widely used because of their high mechanical properties and commercial availability, but their fatigue response changes significantly depending on operating temperature [10]. Recent investigations have examined different alternatives, such as biocomposite gears. Their performance is compared with that of metallic gear systems or other biocomposite-based gears, suggesting that the results are highly dependent on the loading conditions and the main damage mechanism, fatigue or wear mechanisms[11].



Regarding thermal stresses, some studies show that in applications where there are thermal gradients or coupled thermomechanical effects, these thermal stresses can significantly affect the load distribution in the stress-strain state in transmissions [12], so when they are applied, thermal effects must be taken into account.

Recent investigations in helical gear design demonstrate that specific geometric parameters and operating conditions can significantly alter local stress levels [13]; therefore, numerical analysis must be aligned with the gear type, whether spur, helical, or bevel, and with the loading regime of the real system. In contact problems between solids, studies have shown that variables such as the coefficient of friction and geometric ratio directly affect the equivalent plastic strain (PEEQ) during contact [14], which is consistent with the sensitivity of contact phenomena to tribological parameters that, in polymers, are often uncertain unless they are experimentally measured for the specific material pair and operating condition. On the other hand, the design of micro-transmissions and micro-gearboxes has driven the development of advanced methodologies that combine simulation, multi-objective optimization, and validation [2], providing reproducible tools to structure workflows for the design of compact low-torque transmissions. Innovative non-conventional design approaches, for example, those inspired by natural logarithmic curves, have also been proposed to explore new meshing characteristics aimed at performance optimization [15]. In practical situations where it is necessary to quantify geometric degradation due to service, reverse engineering processes for non-standard and worn gears have been evaluated [16], linking wear theory with the direct measurement of geometric changes.

At the manufacturing and material selection level, there are active lines of research focused on the characterization and testing of materials intended for Additive Manufacturing (AM) [17], which is relevant when functional prototypes or production using alternative manufacturing technologies such as FDM/FFF are considered [18]. Studies on parametric optimization of manufacturing processes for load-bearing mechanical components are also reported [19], showing that process parameters directly influence final properties and variability, thereby critically affecting the actual service life of the component in operation. Additionally, changes in the properties of polymeric materials at high temperature are investigated through chemical modifications, for example, grafting [20], demonstrating that the electrical and thermal performance of polymers can be enhanced, although in gear applications, the priority lies in mechanical and tribological attributes. One of the current approaches for metallic gears is the systematic study of processes such as brass waste recycling on their final mechanical properties [21]. This supports the argument that the manufacturing process, including recycling and treatments, impacts the mechanical and tribological performance of the element.

In simulations, different multidomain techniques have been developed to analyze full gearboxes, for example, CFD, which includes gear lubrication or other related fluids [22]. This demonstrates that simulation should not be only focused on the structural aspect but should also incorporate thermal and fluid aspects when required for the design problem. With respect to mechanisms under complicated conditions with many interacting parts, previous studies have used the Finite Element Method (FEM). This method has indicated how mathematical modeling can precisely describe the behavior of interacting bodies [23, 24], confirming the FEM's capacity to precisely determine critical stress zones and transform these stress states into design parameters to evaluate better service life, deterioration, and factors of safety. In conclusion, in fault detection and diagnosis, advanced methods like Lagrange-Wavelet, used in spiral bevel gear systems [25], show that signal analysis techniques complement traditional mechanical analysis to reach consistent degradation detection.

Consequently, the problem addressed in this work is the absence of a structured simulation-based methodology able to relate contact mechanics with both wear evolution and fatigue life evaluation in plastic gear mechanisms under low torque conditions. The originality of this work is the integration of parametric CAD modeling, finite element analysis considering explicit tooth contact, an Archard wear model, and a Stress Life fatigue approach within a single consistent and traceable framework. Additionally, a parametric sensitivity analysis is incorporated to evaluate the impact of uncertain tribological parameters without requiring prior experimental calibration, thereby enhancing the applicability of the methodology for preliminary design and decision-making in compact robotic transmissions.

Based on this comprehensive technical panorama, the present work focuses on the development of a simulation-based analysis methodology for a pair of cylindrical gears, pinion and wheel, oriented toward low-torque robotic applications. The approach integrates parametric CAD with FEM analysis that includes explicit tooth-to-tooth contact [23], in order to: (i) accurately estimate tribological variables associated with flank wear through an Archard-type formulation [3, 6], and (ii) evaluate susceptibility to bending fatigue at the tooth root using a Stress-Life (S-N) approach [4, 10]. The study system is delimited to a spur gear pair as a minimal block that preserves the dominant physics, namely, flank contact leading to wear, root bending leading to fatigue, and heating associated with sliding and friction [3, 4, 5]. To ensure property traceability and analysis reproducibility, a commercial engineering material, PA66 GF30, representative of a glass fiber reinforced polyamide, is selected [10]. Its properties explicitly depend on the material condition, dry or conditioned, and on the reference temperature, aspects that must be stated in the modeling in accordance with technical guidelines [5]. Given the relevance of safe interaction in collaborative robotics, this work is also aligned with safety

and performance guidelines for collaborative robots [26], considering that low-torque transmissions are critical components in applications where the risk of harm during human–robot interaction is minimized. The final objective is to establish a reproducible analysis methodology capable of estimating critical stress fields at the tooth root and contact conditions related to wear, integrating parametric CAD, FEM analysis with explicit contact modeling [23], local mesh refinement in critical regions, namely the root and the flank, and subsequent fatigue life evaluation using an S–N criterion [4, 10], combined with wear assessment through an Archard-type law [3, 6]. The methodology further incorporates parametric sensitivity analysis when uncertain parameters are present, such as the coefficient of friction [14] or the wear coefficient [3]. This workflow aims to provide a reproducible tool that captures sensitivities to tribological uncertainties while simultaneously generating practical design indicators, including Life, Damage, and safety factor, to support decision-making in the development of compact low-torque transmissions [14].

## 2. Methodology

In this research, the methodology is a simulation-based analysis where we estimate (i) the critical stresses at the tooth root, associated with bending fatigue, and (ii) the contact variables relevant to flank wear in a pair of plastic gears, while maintaining traceability of the assumptions and material properties. This research is focused on a pair of cylindrical gears, where we conserve a reduced model that preserves the dominant physics, particularly tooth flank contact, root bending, and the thermal effects associated with friction and sliding motion.

- **Scope and operating assumptions:** In its intended working environment, the robotic system operates under relatively low torque conditions, generally between 0.5 and 10 N·m, with peak values that may reach 10–15 N·m. For polymer-based components, several operating conditions must be considered, such as dry or lubricated contact, reference temperature, and the material condition. (dry or conditioned). In this study, dry operating conditions were assumed; therefore, lubrication effects were not included in the model, and the analysis was carried out using a reference ambient temperature.
- **Parametric CAD design:** The gear geometry was developed as a parametric model in Autodesk Inventor. A spur gear configuration with  $\beta = 0^\circ$  was selected in order to concentrate the analysis on wear and fatigue behaviour. Key geometric variables, including the module, number of teeth, face width, and root fillet radius, were parameterized while ensuring compliance with minimum geometric and assembly requirements.
- **Material:** For this research, we selected the PA66 GF30 material because it is easy to find its traceable data in technical datasheets, and it represents the glass fiber reinforced polyamides very well. To perform the

simulation, only a small group of essential parameters is required, including density, elastic characteristics, an S–N fatigue curve, and a tribological coefficient incorporated into the wear analysis.

- **FEM and failure evaluation:** The geometry is first transferred to ANSYS Mechanical, where the material properties and contact conditions are assigned. A refined mesh is then applied at critical regions, particularly the tooth root and flank surfaces. Once the simulation is completed, stress values at the tooth root and contact-related variables along the flanks, such as normal pressure and sliding behaviour, are obtained. These results are subsequently used as input data for the fatigue evaluation through the S–N curve, as well as for the wear prediction model. Finally, postprocessing tools are employed to automate the parametric assessment and sensitivity analysis of uncertain parameters, including friction and wear-related properties. This procedure makes it possible to identify the dominant failure mechanism within the previously defined low torque operating range.

## 3. Development

### 3.1. Gear Pair Sizing

In this study, we use a cylindrical spur gear pair (a pinion and a wheel) to simulate a compact transmission system for low-torque robotic applications. We focused on flank interaction to evaluate wear and tooth root flexure to evaluate fatigue. The first dimensions were calculated using the spur gear generator in Autodesk Inventor. You can see the CAD model of this assembly in Figure 1.

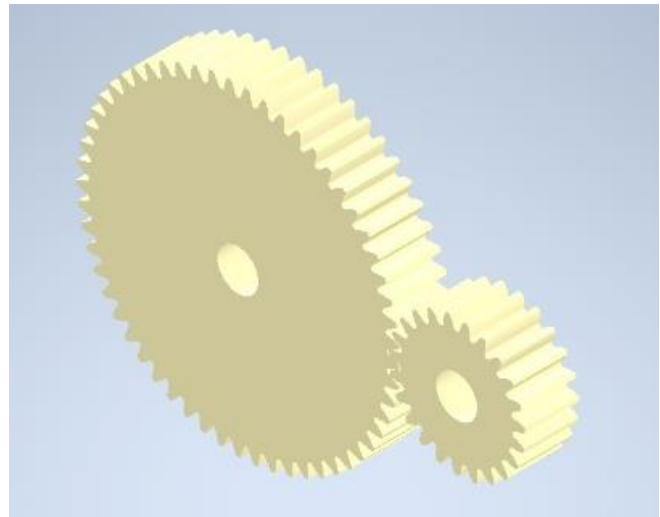


Fig. 1 CAD model of the spur gear pair (pinion–wheel)

We include the geometric characteristics for the reference case, which is shown in Table 1. This considers the module, number of teeth, transmission ratio, center distance, face width, and angle values. We use this table as a primary reference for subsequent simulations.

**Table 1. Geometric parameters**

Parameter	Symbol	Value
Module	$m$	2 mm
Pinion teeth	$z_1$	23
Gear teeth	$z_2$	57
Transmission ratio	$i = \frac{z_2}{z_1}$	2.4783
Center distance	$a$	80 mm
Face width	$b$	20 mm
Pressure angle	$\phi$	20°
Helix angle	$\beta$	0°

**3.2. Loading Conditions**

The simulation is defined from the parameters obtained from the simulator's calculation environment, using the DIN 3990:1988 method, with torque and rotational speed of the pinion shaft as the principal variables. Kinematic consistency

is validated with the transmission—ratio defined in the CAD model. Initially, the pinion works at 1000 rpm with an approximate torque of 10 N·m, while the gear operates at approximately 403.5 rpm and 24.8 N·m, corresponding to  $i \approx 2.478$ .

The transmitted mechanical power is related to torque and rotational speed by [27]:

$$P = \frac{2\pi nT}{60} \tag{1}$$

where P is the power in watts, n is the rotational speed in rpm, and T is the torque in N·m. The load and kinematic verification for the baseline case is shown in Figure 2, and the geometric parameterization of the gear pair in Inventor is shown in Figure 3.



**Fig. 2 Kinematic verification of the train (DIN 3990) and pass parameters for the initial case (P, n, T).**

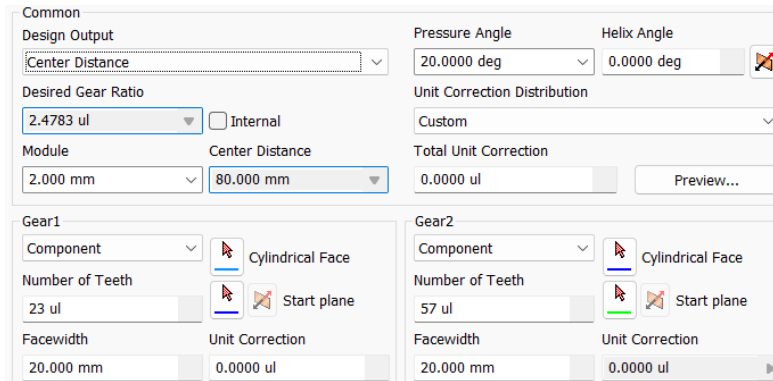


**Fig. 3 CAD parameterization of the spur gear assembly using Autodesk Inventor (m, z, a, b, φ, β).**

**3.3. Material Selection**

For the pinion-wheel assembly, a polyamide 66 material reinforced with 30% glass fiber (PA66-GF30), specifically Ultramid A3WG6 LT BK, was selected because it provides the declared mechanical properties at 23°C under "dry" and conditioned conditions, allowing for the traceability of the numerical model's input data.

In this work, the corresponding PA66\_GF30 material is defined with a density of 1366 kg/m<sup>3</sup> and a tensile modulus of 6800 MPa (23 °C, "cond.").

The properties used include material density, elasticity modulus, tensile property, strain at break, and flexural characteristics, together with their. Respective standards are presented in Table 2, which is used for the contact and wear simulations and evaluation of fatigue.

**Table 2. PA66 GF30 material properties**

Property	Standard	Value (cond., 23 °C)
Density $\rho$ (kg/m <sup>3</sup> )	ISO 1183	1366
Tensile modulus $E$ (MPa)	ISO 527-1/-2	6800
Tensile strength at break (MPa)	ISO 527-1/-2	127
Strain at break (%)	ISO 527-1/-2	6.5
Flexural modulus (MPa)	ISO 178	6500
Flexural strength (MPa)	ISO 178	205

### 3.4. Wear Analysis

- Definition of regions and contact: For load transfer and the extraction of tribological variables, surfaces were

defined using Named Selections, separating the pinion bore as the excitation, the gear bore as the support, and the flanks for tooth-to-tooth contact, as shown in Figure 4.

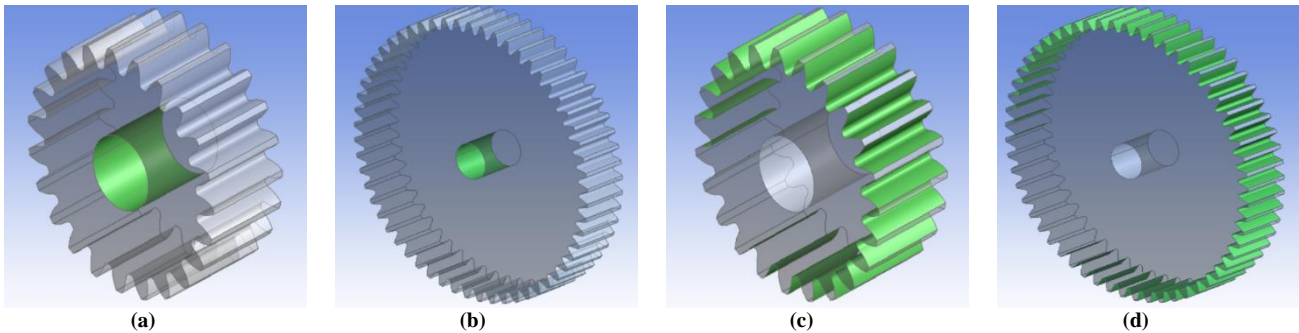


Fig. 4 Scoping surfaces for the model: (a) PINION\_BORE, (b) GEAR\_BORE, (c) PINION\_FLANKS, (d) GEAR\_FLANKS.

The contact was defined between PINION\_FLANKS as the contact surface and GEAR\_FLANKS as the target surface, using an Augmented Lagrange formulation with a frictionless

type, as shown in Figure 5, in order to obtain stable fields of normal pressure and relative sliding to feed the wear model.

Scope	
Scoping Method	Named Selection
Contact	PINION_FLANKS
Target	GEAR_FLANKS
Contact Bodies	Pinion_backlash_0p02
Target Bodies	Gear_backlash_0p02
Protected	No
Definition	
Type	Frictionless
Scope Mode	Manual
Behavior	Program Controlled
Trim Contact	Program Controlled
Contact APDL Name	_con57
Target APDL Name	_tgt57
Suppressed	No
Display	
Element Normals	No
Advanced	
Formulation	Augmented Lagrange
Small Sliding	Program Controlled
Detection Method	Program Controlled
Penetration Tolerance	Program Controlled
Normal Stiffness	Program Controlled
Update Stiffness	Program Controlled
Stabilization Damping Factor	0.
Pinball Region	Radius
Pinball Radius	5.e-002 mm

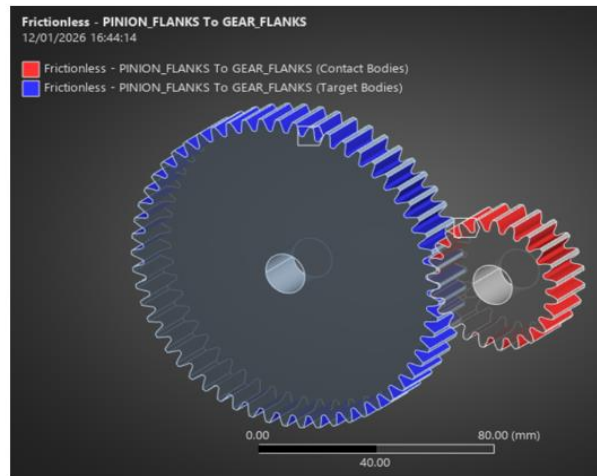


Fig. 5 Definition of tooth-to-tooth contact in ANSYS Mechanical (frictionless, Augmented Lagrange).

- Operating conditions and meshing: The transient analysis in ANSYS was excited with a rotational speed of 1000

rpm and an applied moment of 24,800 N·mm, as illustrated in Figure 6.

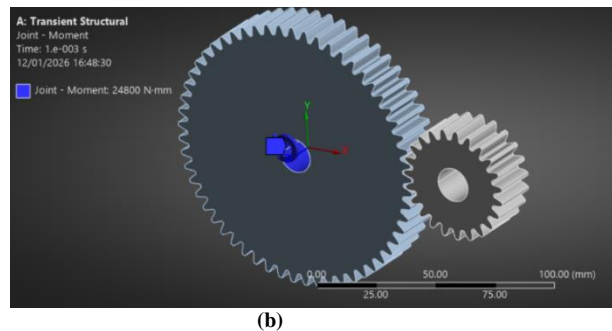
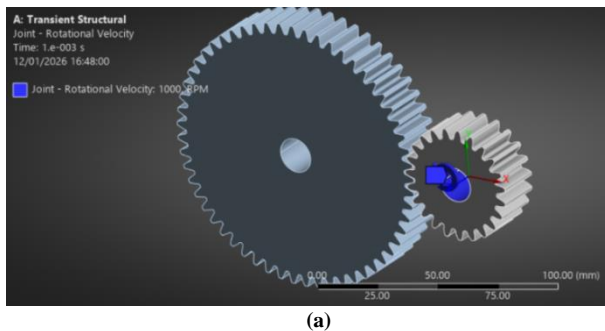


Fig. 6 Transient analysis excitation: (a) Joint – Rotational Velocity (1000 rpm), (b) Joint – Moment (24800 N·mm).

The discretization was carried out using a 3D mesh of the assembly with local refinement to accurately represent the contact patch on the flank, as shown in Figure 7, since pressure and sliding are strongly dependent on the resolution at the interface.

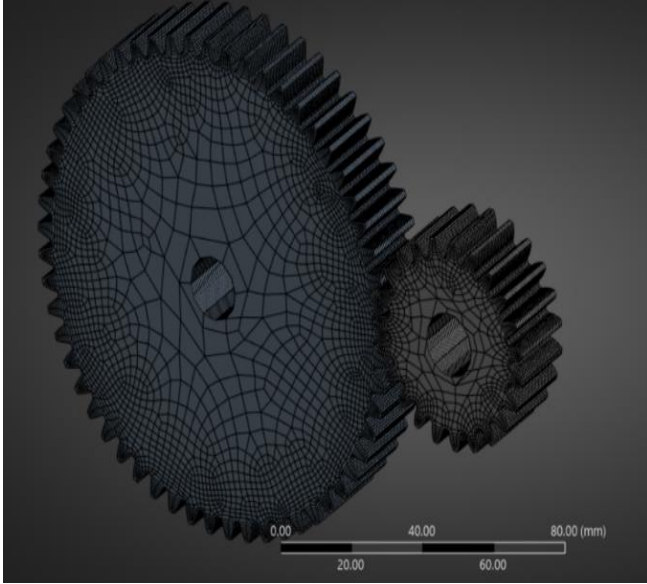


Fig. 7 Mesh of the pinion-wheel assembly used in the transient analysis

- Wear model and input variables: Flank wear was estimated using an integrated Archard-type formulation, employing as FEM inputs the normal contact pressure  $p$  and the sliding increment  $\Delta s$  along the flank. In order to decouple the extraction of FEM fields from the tribological uncertainty of the material pair, an accumulated severity index was defined [28]:

$$I(t) = \sum_{k=1}^{N(t)} p_k \Delta s_k \quad (2)$$

and the wear depth. The relationship between contact severity and accumulated wear is established through a linearized Archard law [29]:

$$h(t) = C_m I(t) \quad (3)$$

where  $C_m$  is an equivalent parameter (1/MPa) that groups the wear coefficient and the effective hardness, this formulation is derived from the differential Archard equation  $dh/ds = k_w \cdot P$  [29], where integration over the sliding distance  $s$  and discretization for cycle-based analysis yield  $h = k_w \cdot P \cdot s$ . By identifying the product  $P \cdot s$  with the severity index  $I(t) = \sum p_k \Delta s_k$  from Eq. (2), and defining  $C_m$  as the dimensional equivalent of  $k_w$ , the compact form  $h(t) = C_m I(t)$  is recovered.

The parameter  $C_m$  is evaluated parametrically, since its value depends on the specific tribological pair, steel and PA66 GF30, and on the operating conditions, dry or lubricated, and temperature. Within this workflow, ANSYS provides  $p(t)$  and  $s(t)$  (or  $\Delta s$  per substep, while MATLAB performs the accumulation to obtain  $I(t)$  and subsequently  $h(t)$  over a range of  $C_m$  values, allowing comparison of scenarios without fixing a single unmeasured value.

### 3.5. Fatigue Analysis

The objective of the fatigue analysis is to estimate the susceptibility to bending failure at the tooth root, specifically in the fillet region, of the pinion-wheel pair, based on the stress state obtained from ANSYS Mechanical and a representative S-N curve for PA66 GF30. The calculation is supported by a prior structural analysis, typically linear static, from which equivalent stresses are extracted for the Stress-Life evaluation.

- Baseline structural case configuration: The load state was defined by a fixed support on the gear, a remote displacement for kinematic control, and an applied moment on the pinion, in accordance with Figure 8.

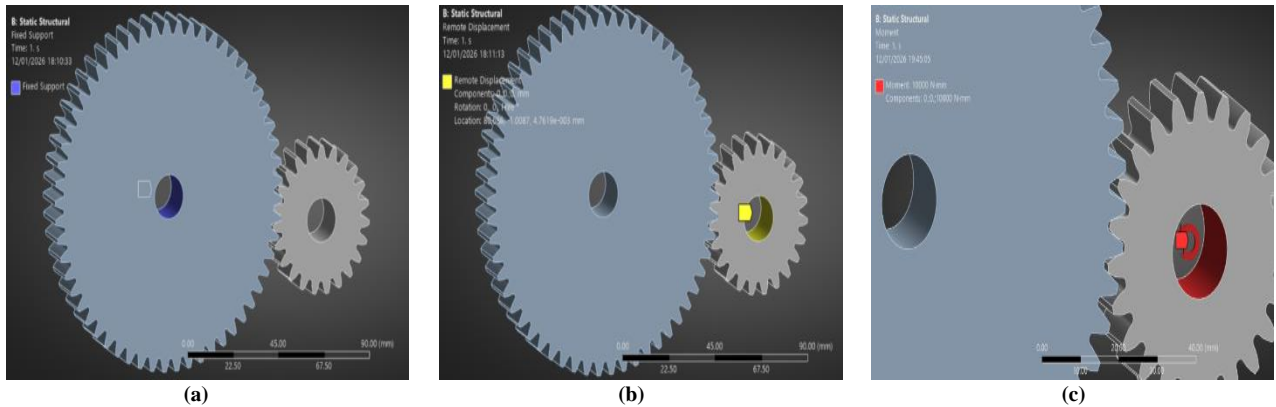


Fig. 8 Boundary and load conditions for the basic structural calculation: (a) Fixed Support type constraint on the wheel, (b) Remote Displacement condition for kinematic control, (c) application of Moment on the pinion.

- Critical region: Due to stress concentration at the root fillet, a specific region was defined for result scoping, PINION\_ROOT\_FILLET\_EDGES, at the pinion tooth root, as shown in Figure 9.

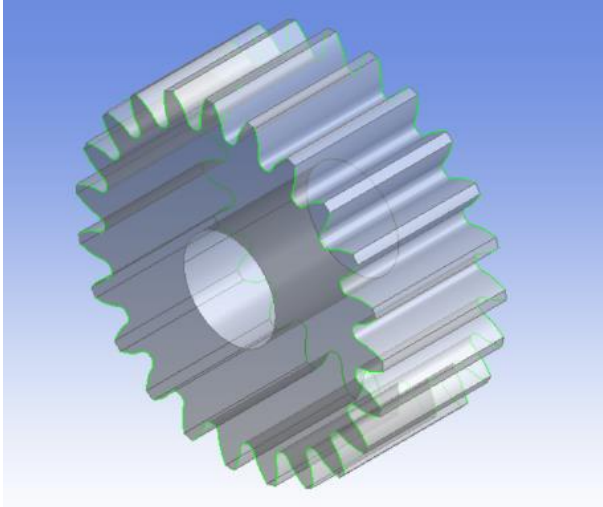


Fig. 9 Critical fatigue assessment region (pinion tooth root): nominal selection PINION\_ROOT\_FILLET\_EDGES to capture bending maxima at the fillet

- S–N curve and traceability: The Stress–Life methodology requires the relationship between alternating stress and cycles to failure, entered as “Alternating Stress vs Cycles” in Engineering Data. In this work, the S–N curve shown in Figure 10 for PA66 GF30 in the high-cycle regime, using a logarithmic scale, was adopted. This curve is used as a reference to compare the equivalent alternating stress calculated by the FEM and to report Life, Damage, and safety factor with respect to a defined Design Life.

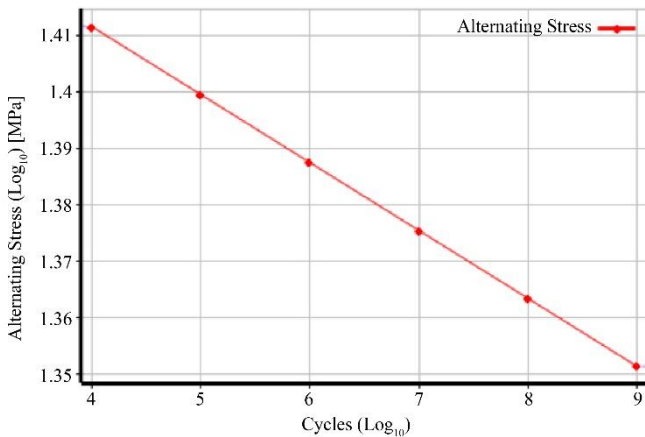


Fig. 10 S–N (Stress–Life) curve of PA66 GF30: alternating stress vs cycles (logarithmic representation) used as input of the fatigue model.

### 3.6. Scaling to Service Conditions (Time–Cycles)

In the transient contact analysis for wear, a short time window is used to sample normal pressure and incremental sliding under operating conditions, whereas fatigue is evaluated with respect to a target life in cycles, referred to as the Design Life. For dimensional consistency, a “cycle” is defined as the repetition of the equivalent load state associated with one revolution of the pinion at the operating speed.

With  $n=1000$  rpm,  $1 \times 10^7$  cycles correspond to approximately  $6.0 \times 10^5$  s of continuous operation under the assumed load state. Under this convention, fatigue results are reported for a Design Life of  $=1 \times 10^7$  cycles, while wear can be scaled by cycle blocks while maintaining the FEM to postprocessing workflow.

Because the simulation is fully deterministic, the outputs rely strictly on the applied boundary conditions and material properties. Consequently, the analysis does not include statistical scatter or error bars. To account for inherent uncertainties in the tribological data, we ran a parametric sweep over the wear coefficients and contact conditions. This approach isolates the sensitivity of the final wear predictions to these specific inputs.

## 4. Results

### 4.1. Wear Analysis

The normal contact pressure field exhibited a localized patch on the flank, with a maximum value of 35.776 MPa at  $t=1 \times 10^{-3}$  s.

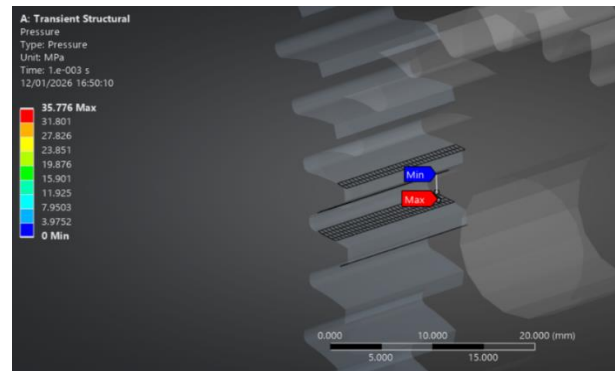


Fig. 11 Flank contact pressure (MPa)

The contact state exhibited regions of sliding and sticking within the active contact patch, as shown in Figure 12.

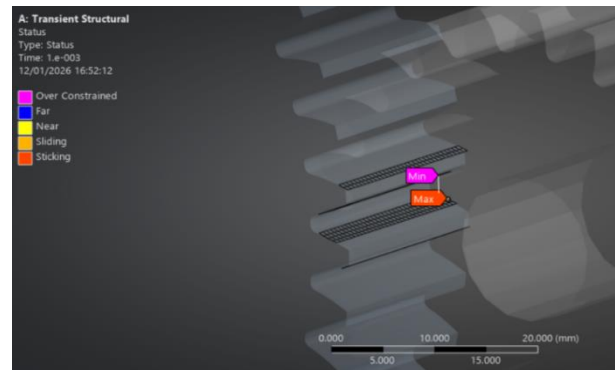


Fig. 12 Contact status on the flank

The accumulated sliding distance reached a maximum of 0.18839 mm at  $t=1 \times 10^{-3}$  s as shown in Figure 13, and was used as the kinematic input for the  $p\Delta s$  integration in the wear model.

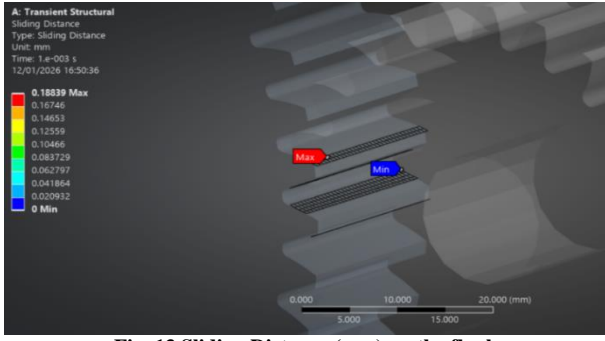


Fig. 13 Sliding Distance (mm) on the flank

From the discrete integration  $I(t)=\sum(p\Delta s)$ , the severity index is reported as  $I_{prom}(t)$  and  $I_{max}(t)$  as shown in Figure 14.

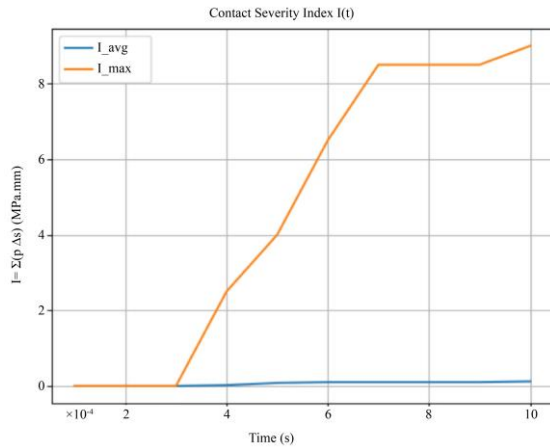


Fig. 14 Contact severity index I(t): comparison between  $I_{prom}$  and  $I_{max}$ .

At the end of the analyzed window, values of  $I_{prom,end}=0.131088$  MPa·mm and  $I_{max,end}=9.13305$  MPa·mm were obtained, as summarized in Table 3. Under a parametric sweep of  $C_m \in [10^{-9}, 10^{-5}]$  1/MPa, the wear depths  $h_{prom}(t)$  and  $h_{max}(t)$  were estimated, as shown in Figures 15 and 16, while maintaining the relation  $h=C_m I$ .

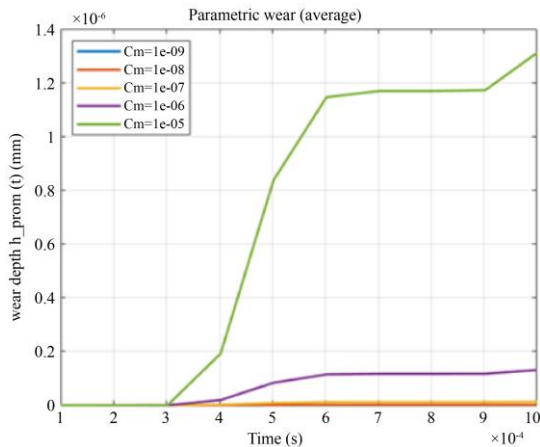


Fig. 15 Average parametric wear  $h_{prom}(t)$  for different  $C_m$

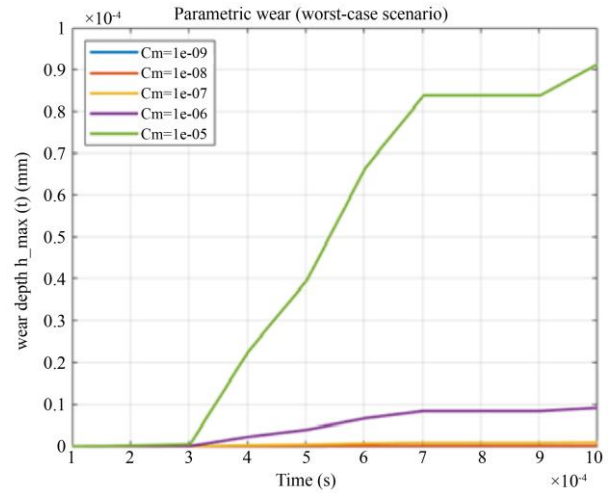


Fig. 16 Worst case parametric wear  $h_{max}(t)$  for different  $C_m$

Table 3. Final values of  $I(t)$  and  $h(t)$  for the  $C_m$  sweep

Parameter		Value
$t_{end}$ (s)		0.001
$I_{avg,end}$ (MPa·mm)		0.131088
$I_{max,end}$ (MPa·mm)		9.13305
$C_m$ (1/MPa)	$h_{avg,final}$ (mm)	$h_{max,final}$ (mm)
$10^{-9}$	$1.3109 \times 10^{-10}$	$9.1331 \times 10^{-9}$
$10^{-8}$	$1.3109 \times 10^{-9}$	$9.1331 \times 10^{-8}$
$10^{-7}$	$1.3109 \times 10^{-8}$	$9.1331 \times 10^{-7}$
$10^{-6}$	$1.3109 \times 10^{-7}$	$9.1331 \times 10^{-6}$
$10^{-5}$	$1.3109 \times 10^{-6}$	$9.1331 \times 10^{-5}$

These results show that  $h_{max}$  increases more rapidly than  $h_{avg}$ , as it is associated with local maxima of contact conditions, namely, pressure and sliding.

The parametric approach allows the prediction of  $h(t)$  to be updated once a traceable value of  $C_m$  becomes available for the specific material pair and tribological condition, dry or lubricated, without modifying the FEM model.

#### 4.2. Fatigue Analysis

The fatigue evaluation for a Design Life of  $1 \times 10^7$  cycles is reported in terms of Life, Damage, and Safety Factor, as shown in Figure 17.

- Life is reported as saturated at  $1 \times 10^9$  cycles, both minimum and maximum values, as shown in Figure 17(a).
- The maximum Damage was  $Damage_{max}=0.01$  as shown in Figure 17(b).
- The minimum safety factor was  $SF_{min}=1.2047$ , located in the critical region at the pinion tooth root, as shown in Figure 17(c).

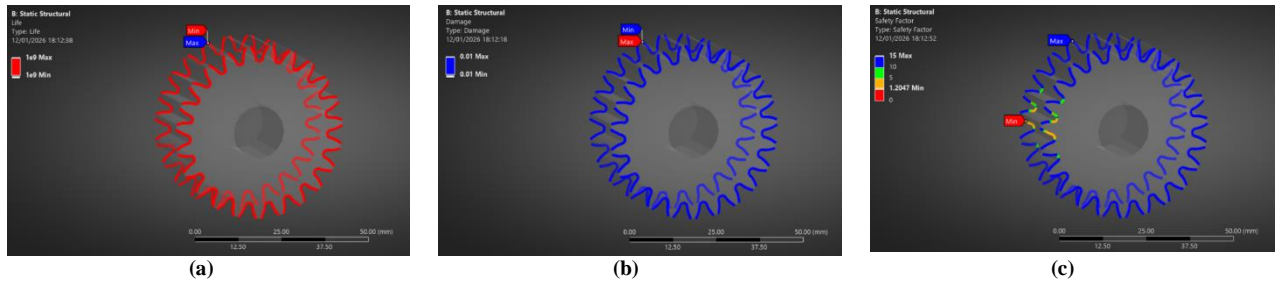


Fig. 17 Stress-Life assessment results for Design Life =  $1e7$  cycles: (a) fatigue life (cycles), (b) fatigue damage (dimensionless) relative to target Life, (c) safety factor relative to target life

For a Design Life of  $=1 \times 10^7$  cycles, values of Damage = 0.01 and  $SF_{min}=1.2047$  were obtained, indicating compliance with the target life under the modeled load state. Given the saturated behavior of Life at  $1 \times 10^9$  cycles, the interpretation of the result is prioritized using Damage and Safety Factor referenced to the specified Design Life.

### 5. Discussion and Practical Implications

The results obtained are clearly applicable to low-torque robotic applications, where compact transmissions, low inertia, and safe human-robot interaction become essential design considerations. Polymer gears made with PA66 GF30 are ideal for collaborative robotic joints, service robots, and lightweight mechanisms or systems requiring moderate load capacity along with high positioning accuracy. What was observed in this study is that the wear and fatigue performance presents a clear view of where the performance limits of these gears are located under the stated operating conditions. Compared with metal gears, these plastic gears present clear advantages: reduced weight, lower operating noise, and improved vibration damping. However, their main limitation is greater sensitivity to environmental and operational conditions, especially temperature and humidity, which can greatly influence their structural rigidity, strength, and wear resistance. The developed approach is ideal for studying these sensitivities by changing parameters, even when it is difficult to incorporate exact conditions in the model.

Regarding durability, wear and flexural fatigue are two mechanisms most likely to control the service life of the analyzed configuration. While it is true that the fatigue analysis indicates acceptable performance within the specified loading conditions, local wear can become a limiting condition when gears are operated for long periods or in unfavorable conditions. This means that it is very important to carefully monitor behavior between gears and load distribution occurring during operation from the design stage. From a fabrication point of view, this methodology is directly applicable to gears produced by traditional injection molding and 3D printing techniques like FDM/FFF. However, designers must take into account that changes in surface quality, internal structure, and material anisotropy associated with each method will affect the gear wear and fatigue

performance. Thus, these manufacturing characteristics must be included in the model when moving to real production conditions.

Concerning sustainability, the polymer part gives notable environmental advantages. Their low-weight nature reduces both material usage and operating energy use in many polymer mixtures. They are fully recyclable. With lifecycle analysis gaining importance in modern engineering, these environmentally friendly characteristics further support the use of plastic gears in compatible mechanical applications. Practically, this simulation approach provides highly valuable information by isolating critical stress zones, defining principal failure modes, and evaluating sensitivity to parameters. Consequently, it makes it possible for design engineers to refine the relationship between geometry, material choice, and operating loads during the preliminary design stage. This proactive approach significantly reduces the reliance on costly and time-consuming physical prototyping.

### 6. Conclusion

- For this study, a tribological workflow was developed to integrate Finite Element (FEM) tooth contact simulations with an Archard-type wear estimation. By utilizing normal contact pressure and relative flank slip as primary inputs, the simulation yielded a pressure of [Variable = 35.776] MPa and a maximum slip distance of 0.18839 at  $t = 1 \times 10^{-3}$  s. These results confirm that the required parameters for the  $p\Delta s$  term in the wear model are successfully available.
- Regarding the stress-life (S-N) fatigue analysis, aimed at a design life of  $10^7$  cycles, a damage fraction of [Variable = 0.01] and a minimum safety factor of [Variable = 1.2047] were recorded at the pinion tooth root. This confirms that the gear can withstand the modeled load for the target lifespan. Since the calculated service life is saturated at  $10^9$  cycles, the interpretations for Damage and safety factor are strictly bounded by the specified design life.
- The obtained results place the minimum safety factor exactly in the expected region for flexural fatigue,

specifically at the tooth fillet and root. This alignment demonstrates that the applied method successfully identifies the critical damage zone and translates raw FEM stress data into practical design metrics, such as service life and safety factors. The safety factor of [Variable] at  $10^7$  cycles indicates an approximate 20% load-bearing reserve against the baseline before structural failure occurs. Consequently, these findings support the use of the selected material and geometry for low-torque applications requiring a similar lifespan. Finally, while the estimated service life is highly dependent on the chosen S-N curve, the overall procedure remains highly adaptable. If material conditions change due to

temperature or humidity, the S-N curve can be updated, allowing the exact same FEM-to-Fatigue workflow to be reused without modifying the analysis structure.

### Conflicts of Interest

The author(s) declare(s) that there is no conflict of interest regarding the publication of this paper.

### Funding Statement

The development of this article is not part of any project; it was self-financed.

## References

- [1] Muhammad Rzi Abbas, Muhammad Ahsan, and Jamshed Iqbal, "Experimental Development of Lightweight Manipulators with Improved Design Cycle Time that Leverages Off-the-Shelf Robotic Arm Components," *PLoS One*, vol. 19, no. 7, pp. 1-32, 2024. [[CrossRef](#)] [[Google Scholar](#)] [[Publisher Link](#)]
- [2] Nikolaos Rogkas et al., "Design, Simulation and Multi-Objective Optimization of a Micro-Scale Gearbox for a Novel Rotary Peristaltic Pump," *Micromachines*, vol. 14, no. 11, pp. 1-19, 2023. [[CrossRef](#)] [[Google Scholar](#)] [[Publisher Link](#)]
- [3] Christoph Herzog, Michael Wolf, and Dietmar Drummer, "In Situ Measured Tooth Flank Wear of Plastic Gears under Spectrum Loading," *Polymers*, vol. 14, no. 23, pp. 1-2022. [[CrossRef](#)] [[Google Scholar](#)] [[Publisher Link](#)]
- [4] Huaiju Liu et al., "Gear Contact Fatigue: Models and Tests," *Friction*, vol. 14, no. 1, pp. 1-24, 2026. [[CrossRef](#)] [[Google Scholar](#)] [[Publisher Link](#)]
- [5] Verein Deutscher Ingenieure, "Thermoplastic Gear Wheels—Materials, Material Selection, Production Methods, Production Tolerances, Form Design," *VDI Guidelines*, 2016. [[Google Scholar](#)] [[Publisher Link](#)]
- [6] Jadwiga Pisula et al., "An Analysis of Polymer Gear Wear in a Spur Gear Train Made Using FDM and FFF Methods Based on Tooth Surface Topography Assessment," *Polymers*, vol. 13, no. 10, pp. 1-20, 2021. [[CrossRef](#)] [[Google Scholar](#)] [[Publisher Link](#)]
- [7] Sándor Bodzás, "Tooth Contact Analysis of Helical Gears Having Modified Straight Teeth by Changing of the Number of Teeth on the Pinion," *Strojnícky Časopis – Journal of Mechanical Engineering*, vol. 70, no. 1, pp. 1-16, 2020. [[CrossRef](#)] [[Google Scholar](#)] [[Publisher Link](#)]
- [8] D. Changbin, L. Yongping, and W. Yongqiao, "Meshing Error of Elliptic Cylinder Gear Based on Tooth Contact Analysis," *International Journal of Engineering, Transactions A: Basics*, vol. 33, no. 7, pp. 1364-1374, 2020. [[CrossRef](#)] [[Google Scholar](#)] [[Publisher Link](#)]
- [9] Y. Koch et al., "A Review on the Use of Angle Measurements in Gear Condition Monitoring and Fault Detection," *Mechanical Systems and Signal Processing*, vol. 225, pp. 1-19, 2025. [[CrossRef](#)] [[Google Scholar](#)] [[Publisher Link](#)]
- [10] Marko Zadavec et al., "Fatigue Behaviour of PA66 GF30 at Different Temperatures," *Polymers*, vol. 17, no. 1, pp. 1- 2025. [[CrossRef](#)] [[Google Scholar](#)] [[Publisher Link](#)]
- [11] Matija Hriberšek, Simon Kulovec, and Lotfi Toubal, "Performance Evaluation of Biocomposite Gears Under Fatigue and Wear: Steel Drive Gear Versus Biocomposite Drive Gear and Biocomposite Drive Gear Versus Biocomposite Gear," *Fatigue & Fracture of Engineering Materials & Structures*, vol. 48, no. 4, pp. 1768-1781, 2025. [[CrossRef](#)] [[Google Scholar](#)] [[Publisher Link](#)]
- [12] Milan Vasić et al., "The Influence of Thermal Stresses on the Load Distribution and Stress–Strain State of Cycloidal Reducers," *Applied Sciences*, vol. 15, no. 17, pp. 1-22, 2025. [[CrossRef](#)] [[Google Scholar](#)] [[Publisher Link](#)]
- [13] Ali Raad Hassan et al., "High-Speed Helical Gear Design Parameters Effect on the Dynamic Stress," *Mathematical Modelling of Engineering Problems*, vol. 10, no. 4, pp. 1189-1198, 2023. [[CrossRef](#)] [[Google Scholar](#)] [[Publisher Link](#)]
- [14] M. Danny Pratama Lamura et al., "Diameter Ratio and Friction Coefficient Effect on Equivalent Plastic Strain (PEEQ) During Contact between Two Brass Solids," *Cogent Engineering*, vol. 10, no. 1, pp. 1-15, 2023. [[CrossRef](#)] [[Google Scholar](#)] [[Publisher Link](#)]
- [15] Jingyu Mo et al., "Aligning Natural Logarithmic Spiral with Gear Drive: How Bionic Gear Design and Characteristics are Affected by Logarithmic Spiral Parameters," *Results in Engineering*, vol. 27, pp. 1-20, 2025. [[CrossRef](#)] [[Google Scholar](#)] [[Publisher Link](#)]
- [16] Karol Konecki, Dominik Wojtkowiak, and Krzysztof Talaška, "Evaluating the Accuracy of the Reverse Engineering Process of Worn, Non-Standard Spur Gears—Pilot Studies," *Applied Sciences*, vol. 14, no. 14, pp. 1-22, 2024. [[CrossRef](#)] [[Google Scholar](#)] [[Publisher Link](#)]
- [17] Alexandr Fales et al., "Innovative Approaches to Material Selection and Testing in Additive Manufacturing," *Materials*, vol. 18, no. 1, pp. 1-30, 2025. [[CrossRef](#)] [[Google Scholar](#)] [[Publisher Link](#)]

- [18] Jarosław Stryczek, Michał Banaś, and Piotr Stryczek, “Research and Development of Fluid Power Elements and Systems Made From Plastics,” *Archives of Civil and Mechanical Engineering*, vol. 25, pp. 1-23, 2025. [[CrossRef](#)] [[Google Scholar](#)] [[Publisher Link](#)]
- [19] Yaroslav Kusyi et al., “Optimization Synthesis of Technological Parameters during Manufacturing of the Parts,” *Maintenance and Reliability*, vol. 24, no. 4, pp. 655-667, 2022. [[CrossRef](#)] [[Google Scholar](#)] [[Publisher Link](#)]
- [20] Xinhua Dong et al., “Improved High-Temperature Electrical Properties of Polypropylene Insulation Material by Grafting Styrene,” *High Voltage*, vol. 10, no. 3, pp. 603-614, 2025. [[CrossRef](#)] [[Google Scholar](#)] [[Publisher Link](#)]
- [21] Erwin Erwin et al., “Effect of the Brass Waste Recycling Process on Mechanical Properties with Investment Casting for Gear Materials,” *Eastern-European Journal of Enterprise Technologies*, vol. 4, no. 12(130), pp. 34-41, 2024. [[CrossRef](#)] [[Google Scholar](#)] [[Publisher Link](#)]
- [22] Marco Nicola Mastrone, and Franco Concli, “A Multi-Domain Modeling Approach for the CFD Simulation of Multi-Stage Gearboxes,” *Energies*, vol. 15, no. 3, pp. 1-16, 2022. [[CrossRef](#)] [[Google Scholar](#)] [[Publisher Link](#)]
- [23] José Ignacio Rojas-Sola, and Juan Carlos Barranco-Molina, “Study of the Mechanical Behavior of a Single-Cylinder Horizontal Steam Engine with a Crosshead Trunk Guide through the Finite-Element Method,” *Applied Sciences*, vol. 14, no. 13, pp. 1-25, 2024. [[CrossRef](#)] [[Google Scholar](#)] [[Publisher Link](#)]
- [24] Tran Huu Danh et al., “Evaluation Strength of Materials of the Compressor Wheel and Engine Power in the Turbocharger,” *Engineering, Technology and Applied Science Research*, vol. 14, no. 4, pp. 15734-15738, 2024. [[CrossRef](#)] [[Google Scholar](#)] [[Publisher Link](#)]
- [25] Ngoc-Duong Nguyen et al., “Diagnosis of Damage in Spiral Bevel Gear Models Using Lagrange–Wavelet Method,” *Advances in Mechanical Engineering*, vol. 16, no. 11, pp. 1-25, 2024. [[CrossRef](#)] [[Google Scholar](#)] [[Publisher Link](#)]
- [26] ISO, *ISO/TS 15066:2016—Robots and Robotic Devices—Collaborative Robots*, 1st ed. Geneva, Switzerland: International Organization for Standardization, 2026. [Online]. Available: <https://www.iso.org/standard/62996.html>
- [27] Engineering ToolBox, Torque—Work Done and Power Transmitted, Engineering ToolBox, 2026. [Online]. Available: [https://www.engineeringtoolbox.com/torque-work-power-d\\_1398.html](https://www.engineeringtoolbox.com/torque-work-power-d_1398.html)
- [28] Aljaž Ignatijev, Matej Borovinšek, and Srečko Glodež, “A Computational Model for Analysing the Dry Rolling/Sliding Wear Behaviour of Polymer Gears Made of POM,” *Polymers*, vol. 16, no. 8, pp. 1-15, 2024. [[CrossRef](#)] [[Google Scholar](#)] [[Publisher Link](#)]
- [29] Enis Muratovic et al., “Assessing Wear Coefficient and Predicting Surface Wear of Polymer Gears: A Practical Approach,” *Engineering, Technology and Applied Science Research*, vol. 14, no. 4, pp. 15923-15930, 2024. [[CrossRef](#)] [[Google Scholar](#)] [[Publisher Link](#)]